ISIJ International, Vol. 49 (2009), No. 12, pp. 1914–1919

Characterization of Mechanically Alloyed Powders for High-Cr Oxide Dispersion Strengthened Ferritic Steel

Noriyuki Y. IWATA,[1)] Ryuta KASADA,[1)] Akihiko KIMURA,[1)] Takanari OKUDA,[2)] Masaki INOUE,[3)] Fujio ABE,[4)] Shigeharu UKAI,[5)] Somei OHNUKI[5)] and Toshiharu FUJISAWA[6)]

1) Institute of Advanced Energy, Kyoto University, Gokasho, Uji, Kyoto 611-0011 Japan. E-mail: noriyuki76@iae.kyoto-u.ac.jp
2) Kobelco Research Institute, Inc., 1-5-5 Takatsukadai, Nishi-ku, Kobe 651-2271 Japan.
3) Advanced Nuclear System R&D Directorate, Japan Atomic Energy Agency, 4002 Narita, Oarai, Higashi-ibaraki, Ibaraki 311-1393 Japan. 4) Structural Metals Center, National Institute for Materials Science, 1-2-1 Sengen, Tsukuba, Ibaraki 305-0047 Japan. 5) Graduate School of Engineering, Hokkaido University, N13, W8, Kita-ku, Sapporo 060-8628 Japan.
6) EcoTopia Science Institute, Nagoya University, Furo, Chikusa-ku, Nagoya 464-8603 Japan.

(*Received on June 12, 2009; accepted on August 18, 2009*)

High-Cr oxide dispersion strengthened (ODS) ferritic steel powders with the nominal composition of Fe–16Cr–4Al–0.1Ti–0.35Y_2O_3 in wt% were produced by milling of elemental powders and Y_2O_3 particles in argon atmosphere to investigate changes in the particle properties during mechanical alloying (MA). SEM observation and PSD analysis revealed that the MA powders milled for different times were composed of agglomerated particles having multimodal distributions with substantial size variation ranging from several μm to 350 μm. The mean size of particles rapidly increased at the initial stage of MA, then gradually decreased to 22 μm with increasing milling time up to 48 h, and kept constant thereafter. During milling of the Fe–16Cr–4Al–0.1Ti–0.35Y_2O_3 powder, MA within 6 h had mainly taken place between Fe and Al to form a bcc-Fe(Al) solid solution. The lattice constant of bcc-Fe steadily increased with a drastic increase in the solute concentrations of Cr, Al, and Ti in Fe. Alloying between Fe and alloying elements is almost fulfilled after milling for 48 h. The MA powder milled in air was much smaller than that milled in gaseous argon under the same conditions. Milling in an air atmosphere is effective to reduce the particle size of the ODS ferritic steel powder, although the pickup of oxygen from environment causes too high excess oxygen content.

KEY WORDS: mechanical alloying; ODS ferritic steel powder; milling time; milling environment.

1. Introduction

Development of fuel cladding materials is inevitable for high-burnup operation in next generation of advanced nuclear systems such as super critical water-cooled reactor (SCWR) and lead-bismuth-cooled fast reactor (LFR). The major material requirements for nuclear fuel claddings are: (i) high strength at elevated temperature, (ii) high resistance to irradiation embrittlement and void swelling, (iii) corrosion resistance in high temperature coolant, and (iv) low susceptibility to hydrogen induced cracking (HIC) and irradiation assisted stress corrosion cracking (IASCC), *etc.*

Oxide dispersion strengthened (ODS) ferritic/martensitic (F/M) steels have been developed for applying them as fuel cladding material in sodium-cooled fast breeder reactor (SFR) systems.[1–4)] The 9Cr ODS F/M steels have shown an excellent high-temperature strength and low void swelling.[5,6)] As for irradiation effects on the mechanical properties, recent irradiation experiments clearly showed that the ODS F/M steels were rather highly resistant to neutron irradiation embrittlement at temperatures between 300 and 500°C up to 15 dpa.[7,8)]

A drastic improvement in high-temperature strength of the conventional ODS F/M steels containing chromium ranging from 9 to 12 wt% was attained by dispersing nano-sized oxide particles. The corrosion resistance in high-temperature water environment is, however, significantly reduced by decreasing Cr content, particularly below 13 wt%. Thus, for the previous 9Cr and/or 12Cr ODS F/M steels, the most critical issue for the application to SCWR systems is to improve their corrosion resistance.

For achieving sufficient corrosion resistance in severe environment, a new series of high-Cr ODS ferritic steels have been developed.[9–15)] In our previous works,[12–15)] it was found that the ODS ferritic steels containing 16 to 19 wt% Cr and 4.5 wt% Al showed excellent corrosion resistance in a super critical pressurized water (SCPW) environment (510°C, 25 MPa). In order to overwhelm the requirements for advanced nuclear fuel claddings, "Development of super ODS steels with high-resistance to corrosion towards highly efficient nuclear systems" was started as a national project supported by the Ministry of Education, Culture, Sports, Science and Technology of Japan (MEXT).[16)]

Mechanical alloying (MA) is a useful powder metallurgy processing technique involving mixing, coalescing, fracturing and remixing of powder particles in high-energy ball

mill, and has now become a viable commercial technique to manufacture ODS alloys. It is well known that the material performance of the ODS steels is controlled by the nature and morphology of the oxide particles dispersed in the matrices that is significantly influenced by the processing conditions such as MA and hot extrusion processes.

The contamination of powder particles during MA is a major concern. Recent efforts clearly showed that the high-temperature strength and microstructure can be improved by lowering excess oxygen (Ex.O) content in ODS martensitic steels.[17,18] Where Ex.O is defined as a subtraction of oxygen content in Y_2O_3 powder from the total O content in steel, and oxygen is easily picked up in powder particles during the milling process. That is, the Ex.O content depends on the milling conditions (grinding medium, grinding bowl, milling time, milling intensity, *etc.*) and the atmosphere under which the powder is being milled.

Although the physical and/or chemical properties of high-Cr ODS ferritic steels have been widely examined, there have not yet been enough evaluation studies so far to adequately comprehend the particle properties of each powder produced by MA. In the present study, MA powders for high-Cr ODS ferritic steel were characterized by means of various techniques as a function of milling time. The effects of milling environment on the particle size of MA powders were also investigated to understand the milling process.

2. Experimental Procedure

2.1. Powder Processing

Elemental Fe (*ca.* 220 μm in size), Cr (<250 μm in size), Al (*ca.* 20–30 μm in size), Ti (<150 μm in size) powders, and Y_2O_3 (*ca.* 30 nm in size) particles were used as starting materials in the present study. High-Cr ODS ferritic steel powders with a nominal composition of Fe–16Cr–4Al–0.1Ti–0.35Y_2O_3 in wt% were produced by milling of powder mixtures in argon (Ar; 99.9999% purity) atmosphere. MA was performed in a planetary mill (PM; Pulverisette 5, Fritsch GmbH) using a chrome steel bowl (500 mL in volume) and balls (10 mm in diameter) at a rotational speed of 180 rpm with a ball-to-powder weight ratio of 15 : 1. The duration of repetitive MA conducted at a milling/pausing cycle of 60/15 min was between 3 and 96 h except for the pausing time. The rotational direction of grinding bowl was alternated between clockwise and counterclockwise at each cycle. All the powder handling was done in a glove box under Ar to prevent the excessive oxidation of the powder particles before and after milling. In order to investigate the effect of milling environment on the MA powder, additional milling was also carried out in air under the same conditions.

2.2. Powder Characterization

The morphology and size of the powders were observed by a scanning electron microscope (SEM; VE-9800, KEYENCE Co.). The particle size distribution (PSD) was measured by a laser diffraction particle size analyzer (LDPSA; LS 230, Beckman Coulter, Inc.) with a small volume module. The crystal structure was examined using an X-ray diffractometer (XRD; RINT-2500VHF, Rigaku Co.) with Cu$K\alpha$ radiation (λ=0.15405 nm) operated at 50 kV and 300 mA. Since the matrix of the powder is a cubic crystal structure, the lattice constant, a, was calculated by substituting lattice spacing, $d_{(hkl)}$, into the following equation.

$$a = \sqrt{h^2 + k^2 + l^2} \cdot d_{(hkl)} \quad \text{.....(1)}$$

An accurate lattice constant was obtained from the intercept of the linear extrapolation of $\cos^2\theta$. A cross-section sample of powder particles was prepared by a cross section polisher (CP; SM-09010, JEOL Ltd.) using Ar ion beam, coated with platinum on the surface, and then investigated by a field emission electron probe microanalyzer (FE-EPMA; JXA-8500FK, JEOL Ltd.) and a high-resolution SEM. The oxygen content in MA powders milled in gaseous Ar and air was also analyzed by an oxygen/nitrogen determinator (TC-436AR, LECO Co.).

3. Results and Discussion

3.1. Effects of Milling Time on Particle Size

The SEM photomicrographs of MA powders milled for different times are shown in **Fig. 1**. The initial powder mixture before milling naturally consists of each raw powder particle, *i.e.*, blocky and flat Fe particles, large Cr particles, fine Al particles with smooth surfaces, spherical Ti particles, and tiny needle-like Y_2O_3 particles, with different particle size and shape. After milling for 3 h, it is obvious that the average size of small and very fine particles increased due to agglomeration of the primary particles into larger

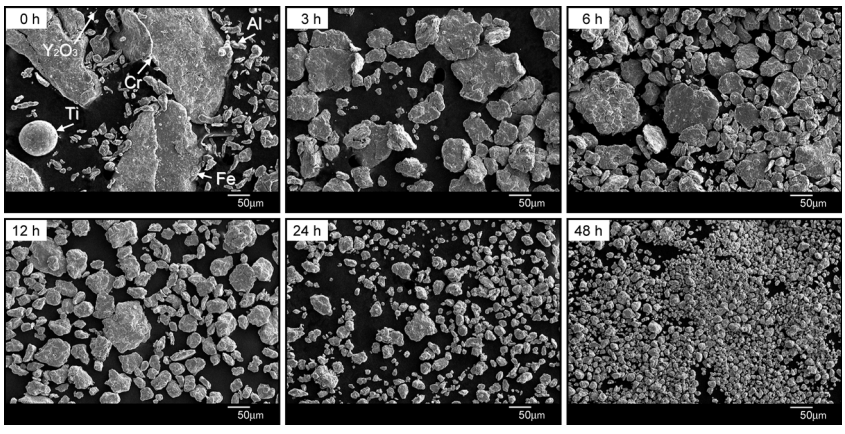

Fig. 1. SEM photomicrographs of MA powders milled for different times in Ar atmosphere.

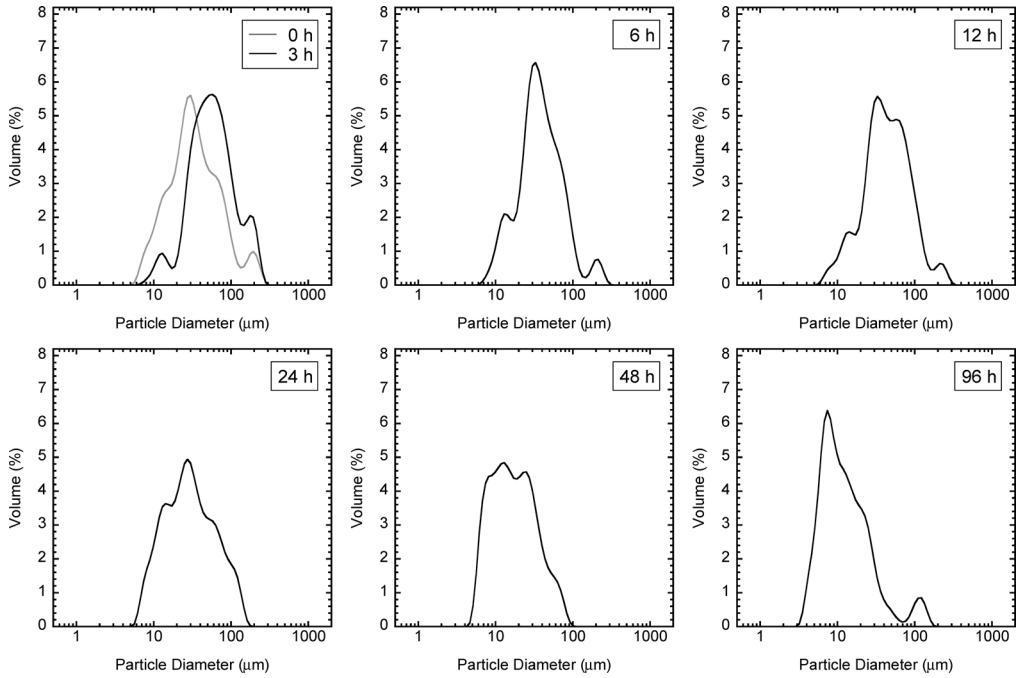

Fig. 2. PSD profiles of MA powders milled for different times in Ar atmosphere.

secondary particles, whereas the size of blocky particles clearly decreased and became irregular in shape. Almost the same trend can be observed in the MA powder milled for 6 h. These trends are quite similar to the results reported in our previous works.[10,11] Beyond 12 h of milling, the apparent size of particles gradually decreased with increasing milling time up to 48 h. It is considered that the secondary particles in the MA powders milled beyond 12 h become work-hardened and get brittle to crush into small fragments.

PSD analyses, before and after milling of the powder mixtures, were carried out by laser diffraction method. As shown in **Fig. 2**, the simply well-blended powder before milling has a multimodal distribution peaking at around 10, 15, 30, 60, and 200 μm, respectively. After milling for 3 h, the obtained PSD profile of the MA powder showed apparently a trimodal distribution and the highest peak position shifted to a larger size as compared to that of the unmilled powder. This is considered to be due to interparticle agglomeration, as evidenced in the SEM image (Fig. 1). After milling for 6 h, the highest peak clearly narrowed and moved to a slightly smaller size in contrast to the MA powder milled for 3 h. The PSD profiles of the MA powders milled beyond 12 h gradually shifted to smaller sizes with increasing milling time and the largest particle diameter of the MA powder milled for 48 h became less than 100 μm. On the contrary, it is found that some coarse particles (*ca.* 100–200 μm in diameter) probably caused by interparticle reagglomeration are present in the MA powder milled for 96 h. The mean particle size of each powder before and after MA was determined by performing the said PSD analysis and also represented in **Fig. 3** as a function of milling time. The mean size of particles rapidly increased at the initial stage of MA and reached to a maximum value of 74 μm after milling for 6 h. Beyond 12 h of milling, the obtained value gradually decreased to 22 μm with increasing milling time up to 48 h and became constant thereafter.

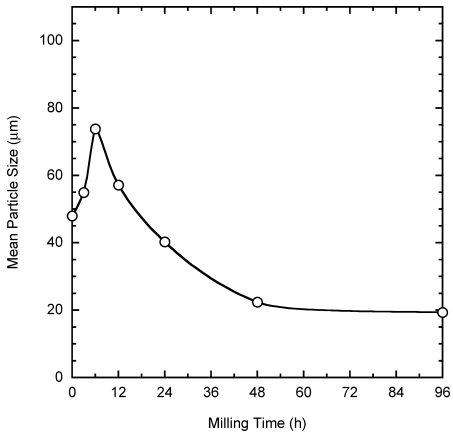

Fig. 3. Mean particle size of MA powders as a function of milling time.

3.2. Examinations by X-ray Diffraction

The effects of milling time on the crystal structure of the powders were examined by powder XRD method. **Figure 4** presents the XRD patterns of MA powders milled for different times. In the powder mixture before milling, the diffraction peaks of Fe, Cr, Al, and Y_2O_3 were detected but no Ti peak was observed because of its low concentration. The Cr (110) peak overlapped with the Fe (110) peak and, furthermore, the Al (200), (220), and (222) peaks overlapped with the Fe (110), (200), and (211) peaks, respectively. After milling for 3 h, the strongest Fe (110) peak became asymmetric and broad, accompanied by a small peak shift to a lower angle than that of the unmilled powder. In addition to that all the Al and Y_2O_3 peaks had almost disappeared. This is considered to be due to introduction of internal strains, dissolution of alloying elements into Fe, and amorphization of Y_2O_3 particles. Moreover, it should be noted that the strongest peak became symmetric after milling for 6 h. With further milling, all the diffraction

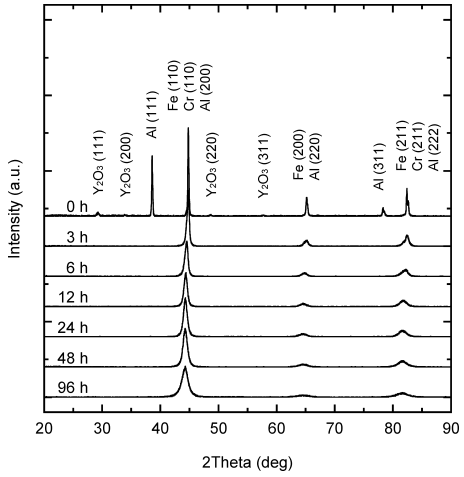

Fig. 4. XRD patterns of MA powders milled for different times in Ar atmosphere.

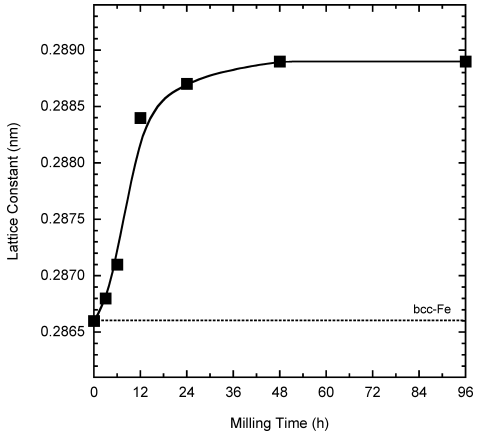

Fig. 5. Lattice constant of bcc-Fe in MA powders as a function of milling time.

peaks became broader and shifted to smaller angles.

Using the peak positions of Fe (110), (200), and (211) in the XRD patterns, an accurate lattice constant of each powder before and after MA was obtained by using the extrapolation method explained above, and shown in **Fig. 5** as a function of milling time. The lattice constant of bcc-Fe drastically increased within 12 h and became saturated after milling for 48 h. It is well known that the dissolution of Al into bcc-Fe results in an increase in the lattice constant of bcc-Fe. As clearly seen in Fig. 4, no diffraction peak of Al was observed in the XRD patterns even after milling for 3 h. The lattice constant of the MA powder milled for 6 h is 0.2871 nm. This is in well agreement with that of bcc-Fe(Al), as observed in the Fe–28Al (*ca.* 16 wt% Al) powder milled for 5 h.[19] These facts prove that MA within 6 h had mainly taken place between Fe and Al to form a bcc-Fe(Al) solid solution. It is also worth noting that the lattice constant of the MA powder milled for 48 h is 0.2889 nm. According to the Vegard's law describing a lattice constant of solid solutions as a linear function of their component contents,[20–22] the relationships between the lattice dilation, Δa, of Fe(M) (M=Cr, Al, and Ti) and the weight percentage concentration of Cr, Al, and Ti in Fe(M), x, can be described as follows:

$$\Delta a_{(\mathrm{Cr})} = 0.000059x\,(\mathrm{wt\%\ Cr})\,\mathrm{nm} \quad \text{.....(2)}$$

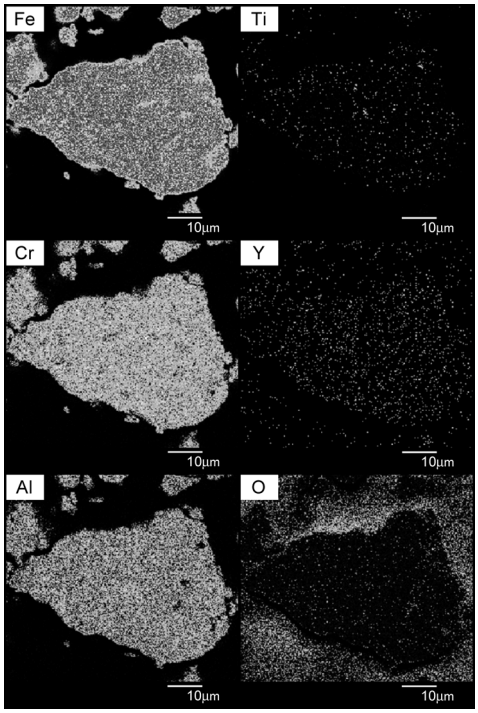

Fig. 6. Cross-section EPMA elemental mapping images of MA powder milled for 12 h in Ar atmosphere.

$$\Delta a_{(\mathrm{Al})} = 0.00033x\,(\mathrm{wt\%\ Al})\,\mathrm{nm} \quad \text{.....(3)}$$

$$\Delta a_{(\mathrm{Ti})} = 0.00036x\,(\mathrm{wt\%\ Ti})\,\mathrm{nm} \quad \text{.....(4)}$$

Therefore, the lattice constant, a, of Fe(M) is:

$$a_{(\mathrm{Fe(M)})} = 0.2866 + \Delta a_{(\mathrm{Cr})} + \Delta a_{(\mathrm{Al})} + \Delta a_{(\mathrm{Ti})}\,\mathrm{nm} \quad \text{.....(5)}$$

If all of the Cr, Al, and Ti atoms enter into the bcc-Fe lattice, the value of a is estimated to be 0.2889 nm (approach to 16 wt% Cr, 4 wt% Al, and 0.1 wt% Ti). This value is equal to those of the MA powders milled for 48 and 96 h. The results show that after milling for 48 h, most of the Cr, Al, and Ti atoms diffuse into the bcc-Fe lattice to form bcc Fe-based solid solutions. As the milling time increases, the solute concentrations of alloying elements in Fe is not apparently changed thereafter, which indicates that the alloying process in the initial target composition was approaching its completion.

3.3. Cross-section Microstructure of Particles

Figure 6 presents the cross-section EPMA elemental mapping images of MA powder milled for 12 h. A particular region rich in Ti is present in the powder particles, whereas Al and Y elements are relatively homogeneously distributed in the Fe matrix. In addition to the alloying elements provided from each raw powder, a small amount of O was detected in the particles, although no clear peak attributed to oxide compounds was observed in the XRD data as shown in Fig. 4. These results indicate that compositional homogeneity of the MA powder is not so high at this stage of milling. In addition to this, the high-resolution cross-section SEM photomicrograph of powder particle after milling for 12 h is shown in **Fig. 7**. A multi-lamellar structure was well developed in the particle having pores ($<1\,\mu$m in diameter). This is obviously due to mechanical deformation

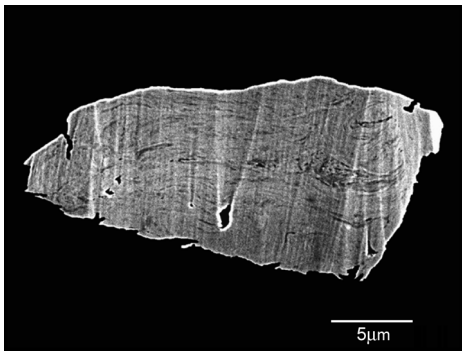

Fig. 7. High-resolution cross-section SEM photomicrograph of powder particle after milling for 12 h in Ar atmosphere.

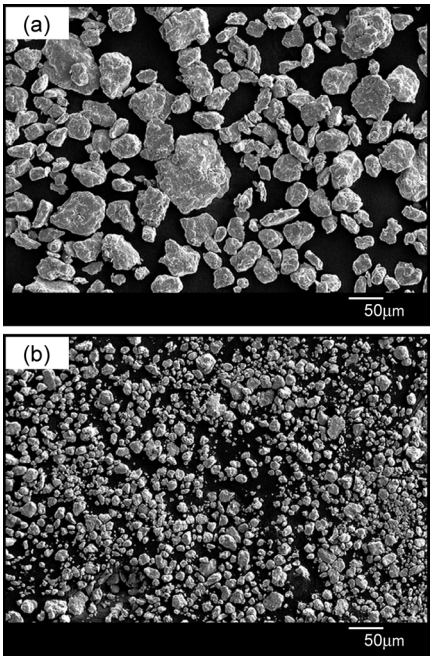

Fig. 8. SEM photomicrographs of MA powders milled for 12 h in (a) gaseous Ar and (b) air atmospheres.

and welding of work-hardened particles, as the powder is vigorously subjected to repeated impacts in the grinding bowl containing a number of balls during milling. Some cracks can also be seen in the interior of the MA powder, which is considered to be caused by intense fracturing effects that occur during this milling stage.

3.4. Effects of Milling Environment on Particle Size

Two types of MA powders were produced in different atmospheres under the same conditions to investigate the influences of milling environment on the particle size. The SEM photomicrographs of the each powder milled for 12 h in (a) gaseous Ar and (b) air are shown in **Fig. 8**. At first glance, the MA powder milled in air has much more small-scale particles than that milled in Ar. Highly agglomerated particles in each powder can be observed here as well. Oxygen analyses showed that the oxygen contents are 0.48 and 1.17 wt% for the MA powders milled in Ar and air, respectively.

Figure 9 presents the PSD profiles of those powders shown in Fig. 8. The MA powder milled in gaseous Ar has a multimodal distribution ranging from 5 to 350 μm. Meanwhile, the PSD profile of the MA powder milled in air exhibited apparently a trimodal distribution ranging from 3 to 90 μm. The primary peaks obviously shifted to smaller sizes when air atmosphere was used for MA. As for the mean particle size, the obtained values are 57 and 20 μm for the MA powders milled in Ar and air, respectively. These facts prove that milling in air atmosphere considerably reduces the particle size of the ODS ferritic steel powder. The previous work also indicated that the PSD profile of the MA powder milled with the grinding bowl having air leakage was similar to that obtained for the powder milled in air, and the consolidated bulk materials fabricated from the former MA powder had a higher hardness than those fabricated from the powder milled in pure Ar.[23] This suggests that the milling in air results in the hardening or embrittlement of the MA powder, and the larger particles crush into smaller particles.

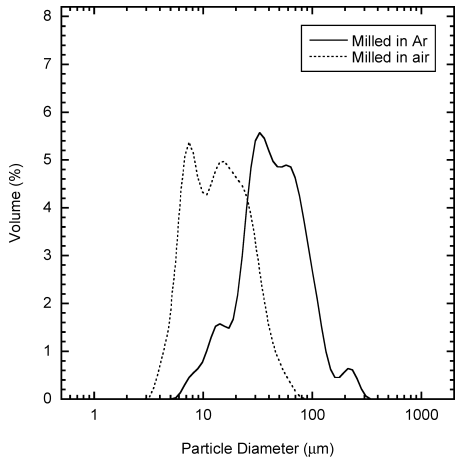

Fig. 9. PSD profiles of MA powders milled for 12 h in different atmospheres.

4. Conclusions

Characteristics of MA powders for high-Cr ODS ferritic steel were extensively investigated to understand the milling process starting from elemental powders and Y_2O_3 particles. The main results are summarized as follows:

(1) The MA powders milled for different times were composed of agglomerated particles having multimodal distributions with substantial size variation ranging from several μm to 350 μm. The mean size of particles rapidly increased at the initial stage of MA, reached to a maximum value of 74 μm at 6 h, then gradually decreased to 22 μm with increasing milling time up to 48 h, and kept constant thereafter.

(2) At the initial stage ($<$6 h) during milling of the Fe–16Cr–4Al–0.1Ti–0.35Y_2O_3 powder, MA between Fe and Al mainly occurred to form a bcc-Fe(Al) solid solution. At the middle stage (6–48 h), the lattice constant of bcc-Fe steadily increased with a drastic increase in the solute concentrations of Cr, Al, and Ti in Fe. At the final stage ($>$48 h), alloying between Fe and alloying elements is almost fulfilled.

(3) The SEM observation and PSD analysis revealed that the MA powder milled in air was much smaller than that milled in gaseous Ar under the same conditions. This

indicates that milling in an air atmosphere is effective to reduce the particle size of the ODS ferritic steel powder, although the pickup of oxygen from environment causes too high excess oxygen content.

(4) From the results thus obtained, it is concluded that the adequate milling time can be determined to be 48 h at a rotational speed of 180 rpm with a ball-to-powder weight ratio of 15 : 1 to attain the minimum size of MA powder for high-Cr ODS ferritic steel, Fe–16Cr–4Al–0.1Ti–0.35Y_2O_3. It is considered that oxygen pickup from environment causes a remarkable particle size reduction of the MA powder.

Acknowledgements

Present study includes the result of "Development of super ODS steels with high-resistance to corrosion towards highly efficient nuclear systems" entrusted to Kyoto University by the Ministry of Education, Culture, Sports, Science and Technology of Japan (MEXT). This work is partly supported by the ISIJ Research Promotion Grant from the Iron and Steel Institute of Japan. The authors are very grateful to Prof. Norimichi Kawashima of the Biomedical Engineering Center, Toin University of Yokohama, Japan, for performing PSD and XRD analyses.

REFERENCES

1) S. Ukai, T. Nishida, H. Okada, T. Okuda, M. Fujiwara and K. Asabe: *J. Nucl. Sci. Technol.*, **34** (1997), 256.
2) S. Ukai, T. Nishida, T. Okuda and T. Yoshitake: *J. Nucl. Sci. Technol.*, **35** (1998), 294.
3) S. Ukai, T. Nishida, T. Okuda and T. Yoshitake: *J. Nucl. Mater.*, **258–263** (1998), 1745.
4) S. Ukai, S. Mizuta, T. Yoshitake, T. Okuda, M. Fujiwara, S. Hagi and T. Kobayashi: *J. Nucl. Mater.*, **283–287** (2000), 702.
5) S. Ukai, T. Narita, A. Alamo and P. Parmentier: *J. Nucl. Mater.*, **329–333** (2004), 356.
6) M. B. Toloczko, D. S. Gelles, F. A. Garner, R. J. Kurtz and K. Abe: *J. Nucl. Mater.*, **329–333** (2004), 352.
7) T. Yoshitake, T. Ohmori and S. Miyakawa: *J. Nucl. Mater.*, **307–311** (2002), 788.
8) A. Kimura, H. S. Cho, J. S. Lee, R. Kasada, S. Ukai and M. Fujiwara: Proc. of 2004 Int. Cong. on Advances in Nuclear Power Plants (ICAPP '04), on CD-ROM, American Nuclear Society, Illinois, USA, (2004), 2070.
9) A. Kimura, H. S. Cho, N. Toda, R. Kasada, H. Kishimoto, N. Y. Iwata, S. Ukai and M. Fujiwara: Proc. of 2005 Int. Cong. on Advances in Nuclear Power Plants (ICAPP '05), Curran Associates, Inc., New York, USA, (2007), 1737.
10) N. Y. Iwata, A. Kimura, S. Ukai, M. Fujiwara and N. Kawashima: Proc. of 2005 Int. Cong. on Advances in Nuclear Power Plants (ICAPP '05), Curran Associates, Inc., New York, USA, (2007), 2721.
11) N. Y. Iwata, A. Kimura, M. Fujiwara and N. Kawashima: *J. Nucl. Mater.*, **367–370** (2007), 191.
12) H. S. Cho, A. Kimura, S. Ukai and M. Fujiwara: *J. Nucl. Mater.*, **329–333** (2004), 387.
13) H. S. Cho, H. Ohkubo, N. Y. Iwata, A. Kimura, S. Ukai and M. Fujiwara: Proc. of 2005 Int. Cong. on Advances in Nuclear Power Plants (ICAPP '05), Curran Associates, Inc., New York, USA, (2007), 2387.
14) H. S. Cho, H. Ohkubo, N. Y. Iwata, A. Kimura, S. Ukai and M. Fujiwara: *Fusion Eng. Des.*, **81** (2006), 1071.
15) H. S. Cho and A. Kimura: *J. Nucl. Mater.*, **367–370** (2007), 1180.
16) A. Kimura, H. S. Cho, N. Toda, R. Kasada, H. Kishimoto, N. Y. Iwata, S. Ukai, S. Ohtsuka and M. Fujiwara: Proc. of 2007 Int. Cong. on Advances in Nuclear Power Plants (ICAPP '07): "The Nuclear Renaissance at Work", Curran Associates, Inc., New York, USA, (2008), 2148.
17) S. Ukai, T. Kaito, S. Ohtsuka, T. Narita, M. Fujiwara and T. Kobayashi: *ISIJ Int.*, **43** (2003), 2038.
18) S. Ohtsuka, S. Ukai, M. Fujiwara, T. Kaito and T. Narita: *J. Nucl. Mater.*, **329–333** (2004), 372.
19) W. M. Tang, Z. X. Zheng, H. J. Tang, R. Ren and Y. C. Wu: *Intermetallics*, **15** (2007), 1020.
20) L. Zwell and H. A. Wriedt: *Metall. Trans.*, **3** (1972), 593.
21) L. Zwell, G. R. Speich and W. C. Leslie: *Metall. Trans.*, **4** (1973), 1990.
22) B. Huang, K. N. Ishihara and P. H. Shingu: *Mater. Sci. Eng. A*, **231** (1997), 72.
23) A. Kimura: Annual Report of the MEXT Innovative Nuclear R&D Program: "Development of Super ODS Steels with High-Resistance to Corrosion Towards Highly Efficient Nuclear Systems", on CD-ROM, Kyoto University, Kyoto, (2007).